Eur. J. Biochem. **268**, 1596–1604 (2001) © FEBS 2001

Biosynthesis of cannabinoids

Incorporation experiments with ^{13}C-labeled glucoses

Monika Fellermeier[1], Wolfgang Eisenreich[2], Adelbert Bacher[2] and Meinhart H. Zenk[1]

[1]*Biozentrum-Pharmazie, Universität Halle, Halle/Saale, Germany;* [2]*Lehrstuhl für Organische Chemie und Biochemie, Technische Universität München, Garching, Germany*

The biosynthesis of cannabinoids was studied in cut sprouts of *Cannabis sativa* by incorporation experiments using mixtures of unlabeled glucose and [1-^{13}C]glucose or [U-$^{13}C_6$]glucose. ^{13}C-labeling patterns of cannabichromenic acid and tetrahydrocannabinolic acid were analyzed by quantitative NMR spectroscopy. ^{13}C enrichments and coupling patterns show that the C_{10}-terpenoid moiety is biosynthesized entirely or predominantly (> 98%) via the recently discovered deoxyxylulose phosphate pathway. The phenolic moiety is generated by a polyketide-type reaction sequence. The data support geranyl diphosphate and the polyketide, olivetolic acid, as specific intermediates in the biosynthesis of cannabinoids.

Keywords: biosynthesis; cannabinoid; deoxyxylulose; NMR spectroscopy; polyketide.

Cannabinoids, a group of terpenophenolics, are accumulated in considerable amounts in glandular trichomes of *Cannabis sativa* (Cannabaceae) [1]. Numerous representatives of this group have been characterized. Because of their psychotomimetic effects, *Cannabis* preparations such as marijuana and hashish, have been used for centuries and are still among the most widely used illicit drugs [2]. Since the discovery of specific receptors for tetrahydrocannabinol in mammalian brain and peripheral tissues, and the isolation of endogenous ligands for these receptors, cannabinoids have attracted renewed interest for medicinal applications including the relief of pain, nausea caused by cancer chemotherapy or acute glaucoma, and the control of spasticity and tremor in patients suffering from multiple sclerosis [3–5], as well as for therapy of arthritis [6].

The biosynthesis of cannabinoids was studied in the 1970s using radiolabeling experiments [7]. Specifically, ^{14}C-labeled mevalonate and malonate were shown to be incorporated into tetrahydrocannabinolic acid (**7**) and cannabichromenic acid (**6**), albeit at low rates (< 0.02%). More recently, it was shown that geranyl diphosphate (**3**) and olivetolic acid (**4**) can be converted by cell extracts of *C. sativa* into cannabigerolic acid (**5**) [8]. Moreover, enzymes catalyzing the formation of tetrahydrocannabinolic acid (**7**), cannabichromenic acid (**6**) or cannabidiolic acid (**8**) from cannabigerolic acid (**5**) have been purified and characterized (Fig. 1) [9–11].

Correspondence to M. Fellermeier: Biozentrum-Pharmazie, Universität Halle, Weinbergweg 22, 06120 Halle/Saale, Germany.
Fax: +49 345 552 7301, Tel.: +49 345 552 5064,
E-mail: zenk@biozentrum.uni-halle.de

Abbreviations: DMAPP, dimethylallyl diphosphate; HMBC, heteronuclear multiple quantum multiple bond correlation; HMQC, hetreonuclear multiple quantum correlation; INADEQUATE, incredible natural abundance double quantum transfer experiment; IPP, isopentenyl diphosphate.

(Received 13 November 2000, accepted 15 January 2001)

Up until 1990, the precursors of all terpenoids, isopentenyl diphosphate (IPP, **1**) and dimethylallyl diphosphate (DMAPP, **2**) were believed to be biosynthesized via the mevalonate pathway. Subsequent studies, however, showed that many plant terpenoids are biosynthesized via the recently discovered deoxyxylulose phosphate pathway which is summarized in Fig. 2 [12,13]. The first intermediate of this alternative terpenoid pathway, 1-deoxy-D-xylulose 5-phosphate (**11**), is formed from D-glyceraldehyde 3-phosphate (**10**) and pyruvate (**9**) by the catalytic action of 1-deoxyxylulose 5-phosphate synthase (dxs protein) and is converted to 2C-methyl-D-erythritol 2,4-cyclodiphosphate (**12**) by the subsequent catalytic action of dxr, ispD, ispE and ispF proteins which have been found in bacteria as well as plants [14]. In higher plants, the two terpenoid pathways appear to be compartmentally separated. Specifically, the deoxyxylulose phosphate pathway appears to operate in the plastid compartment, and the mevalonate pathway is located in the cytoplasm [15,16].

In order to analyse the biosynthetic origin of cannabinoid precursors, cut sprouts of *C. sativa* were proffered with a mixture of unlabeled glucose and [U-$^{13}C_6$]glucose or [1-^{13}C]glucose. Tetrahydrocannabinolic acid (**7**) and cannabichromenic acid (**6**) were isolated and analyzed by quantitative NMR spectroscopy. The data provide clear evidence that the C_5-terpenoid precursors, IPP (**1**) and DMAPP (**2**), are derived predominantly (> 98%) via the deoxyxylulose phosphate pathway. The phenolic moiety of tetrahydrocannabinolic acid (**7**) and of cannabichromenic acid (**6**) was shown to be generated via a polyketide-type mechanism.

MATERIALS AND METHODS

Chemicals

[1-^{13}C]Glucose (99.9% ^{13}C enrichment) and [U-$^{13}C_6$]glucose (99.9% ^{13}C enrichment) were purchased from Cambridge Isotope Laboratories (Woburn, MA, USA).

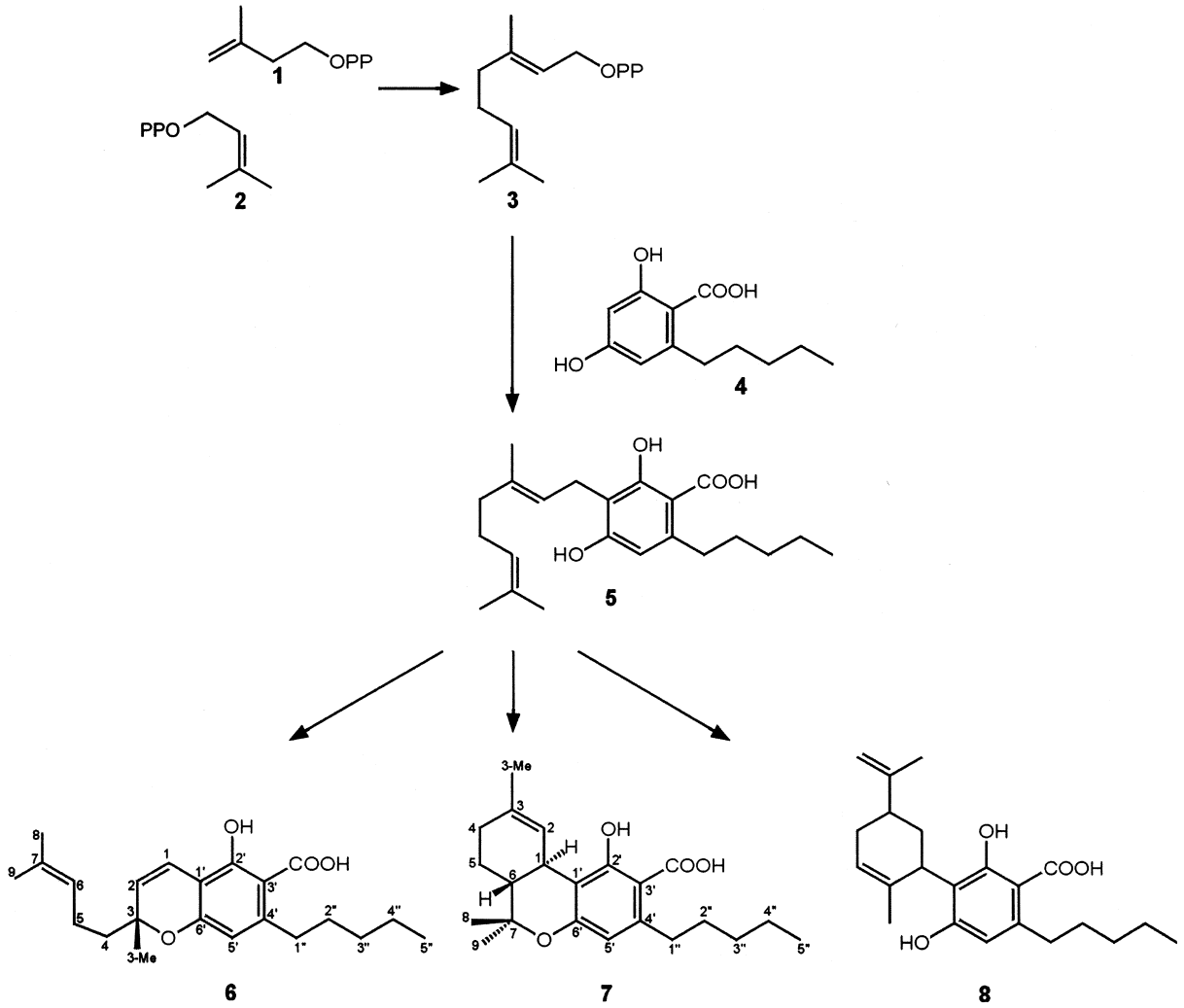

Fig. 1. Biosynthesis of cannabichromenic acid (6), tetrahydrocannabinolic acid (7) and cannabidiolic acid (8) according to published mechanisms [7–11].

Plant material and cultivation

Sprouts containing a leaf bud and 3–5 leaves were cut from female plants of *C. sativa* var. Thai (≈ 24 weeks old) grown in a greenhouse with legal permission. Groups of 20 sprouts were supplied with a solution containing 0.5% (w/w) [1-^{13}C]glucose (99.9% ^{13}C enrichment) and 0.5% (w/w) unlabeled glucose or with a solution containing 0.05% (w/w) [U-$^{13}C_6$]glucose and 0.95% (w/w) unlabeled glucose. The sprouts were incubated for 10 days at 25 °C at a relative humidity of 40–50% and under 14 h light/ 10 h dark conditions. Small sections from the ends of the stems were removed with a razor blade at intervals of 24 h.

Isolation of cannabinoids

The plant material (≈ 35 g fresh weight) was frozen in liquid nitrogen, triturated and extracted with 750 mL of hexane. The extract was filtered and concentrated to a volume of 30 mL. Aliquots (5 mL) were placed on top of Chromabond NH_2 columns (500 mg, Macherey & Nagel) which had been equilibrated with methanol followed by diethyl ether and hexane. The columns were washed with diethyl ether followed by a mixture of chloroform/ isopropanol (2 : 1, v/v, 5 mL) and were then developed with 5 mL of diethyl ether/acetic acid (98 : 2, v/v). The effluent was concentrated to dryness under reduced pressure. The residue was dissolved in 5 mL of methanol. Aliquots of that solution were placed on a column of Lichrosorb RP-18, 7 μm, 25 × 250 mm (Merck) using a solvent system consisting of solvent A (H_2O/acetonitril/ acetic acid, 98 : 1.9 : 0.1, v/v) and solvent B (H_2O/ acetonitril/acetic acid, 1.9 : 98 : 0.1, v/v). A linear gradient of 50–100% of solvent B in A was applied for 90 min, at a flow rate of 10 mL·min^{-1}. The effluent was monitored photometrically. Tetrahydrocannabinolic acid and cannabichromenic acid were eluted at retention times of 55 and 60 min, respectively.

NMR spectroscopy

^{1}H-NMR and ^{13}C-NMR spectra were recorded at 500.13 and 125.6 MHz, respectively, using a Bruker DRX 500 spectrometer. Acquisition and processing parameters for

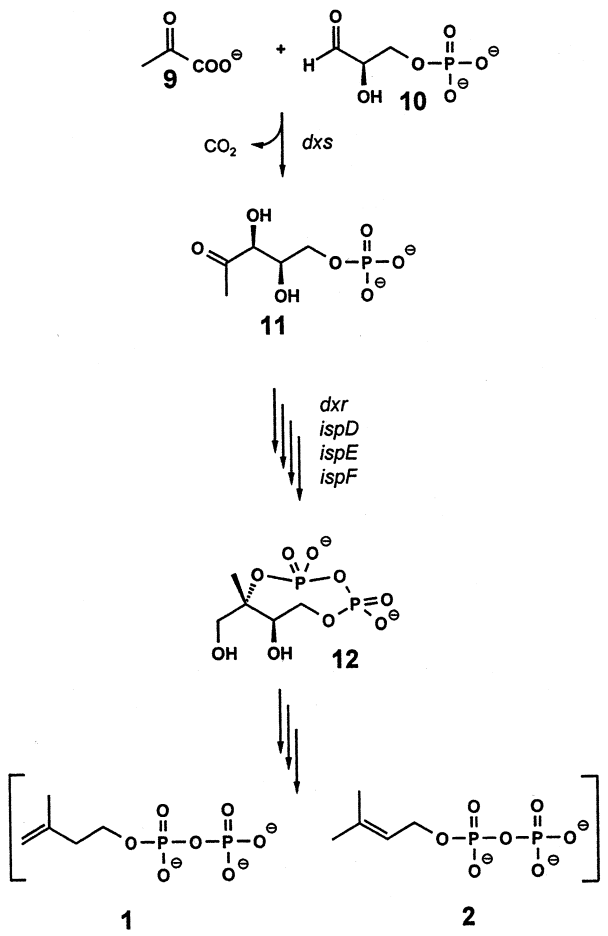

Fig. 2. Biosynthesis of IPP (1) and DMAPP (2) via the deoxyxylulose phosphate pathway [12–14].

one-dimensional experiments and two-dimensional COSY, incredible natural abundance double quantum transfer (INADEQUATE), heteronuclear multiple quantum correlation (HMQC) and heteronuclear multiple quantum multiple bond correlation (HMBC) experiments were according to standard Bruker software (XWINNMR). The solvent was deuterated chloroform. The chemical shifts were referenced to solvent signals.

Determination of ^{13}C labeling patterns

The methods used to determine ^{13}C enrichment have been described in detail previously [17,18]. Briefly, ^{13}C NMR spectra of the isotope-labeled compound under study and of natural abundance material were recorded under the same experimental conditions. Integrals were determined for every ^{13}C NMR signal, and the signal integral for each respective carbon atom in the labeled compound was referenced to that of the natural abundance material, thus affording relative ^{13}C abundances for each position in the labeled molecular species.

In certain instances, these relative abundances can be converted to approximate absolute enrichment by assigning a value of 1.1% to the carbon atom with the lowest ^{13}C enrichment and referencing all other carbons to that position. In other cases, absolute ^{13}C enrichment can be obtained for certain atoms from ^{13}C coupling satellites in ^{1}H NMR spectra provided that any hydrogen atom of the compound under study is a singlet or a doublet in which the coupling satellites can be determined to relatively high accuracy.

In NMR spectra of multiple-labeled samples displaying $^{13}C^{13}C$ couplings, each satellite in the ^{13}C NMR spectra is integrated separately. The integral of each respective satellite pair is then referenced to the total signal integral of a given carbon atom.

RESULTS AND DISCUSSION

Young cut sprouts of *C. sativa* were cultivated in a solution containing 1% (w/w) glucose for 10 days. Tetrahydrocannabinolic acid (120 mg) and cannabichromenic acid (35 mg) were isolated from plant material (fresh weight, 35 g), as described above, and analysed by ^{1}H and ^{13}C NMR spectroscopy. All ^{1}H and ^{13}C NMR signals of cannabichromenic acid (**6**) and tetrahydrocannabinolic acid (**7**) were assigned using two-dimensional homocorrelation (DQF-COSY, NOESY) and heterocorrelation experiments (HMQC, HMBC) (Tables 1 and 2). These assignments were further confirmed by two-dimensional INADEQUATE experiments with the multiply ^{13}C-labeled samples obtained from the experiment with [U-$^{13}C_6$]glucose.

In the experiment with [U-$^{13}C_6$]glucose, the average ^{13}C abundance of all carbon atoms was 1.7 ± 0.1% ^{13}C in **6** and 1.6 ± 0.1% ^{13}C in **7**, i.e. ≈1.5 × the natural level (Table 3). All ^{13}C signals of compound **6** (Fig. 3) and compound **7** showed satellites indicative of $^{13}C^{13}C$ couplings. The relative fractions of satellite signals in the global ^{13}C NMR signal intensities of most atoms was 30–40%, i.e. well above the natural abundance background (1.1% for two contiguous ^{13}C atoms in natural abundance material) (Figs 3 and 4).

The detected ^{13}C signal satellites were attributed to 10 isotopomers of **6** and **7** with adjacent ^{13}C atoms by a detailed analysis of coupling constants, as well as by two-dimensional INADEQUATE experiments (Tables 1 and 2, Fig. 3).

More specifically, six $^{13}C_2$ isotopomers with adjacent ^{13}C atoms were formed in the phenolic ring and the hexyl side chain of **6** resp. **7** (Fig. 5A). Four $^{13}C_2$ isotopomers with contiguous ^{13}C atoms in the terpenoid moieties comprising C-1 to C-9 and the 3-methyl atom were observed. Moreover, the coupling satellites of C-5 and C-6, as well as the signal of C-8 of **6**, showed long-range ^{13}C coupling indicative of [5,6,8-$^{13}C_3$]**6** (Figs 4 and 5A). As outlined in detail below, a $^{13}C_3$-labeled isotopomer cannot be explained by a mevalonate origin of the terpenoid moiety, because only $^{13}C_2$ fragments can be diverted to IPP/DMAPP from [U-$^{13}C_6$]glucose via [U-$^{13}C_2$]acetyl-CoA. In contrast, a triple of ^{13}C atoms from [U-$^{13}C_6$]glucose can be diverted to terpenoid precursors via [U-$^{13}C_3$]glyceraldehyde 3-phosphate by the nonmevalonate pathway of terpenoid biosynthesis.

From [1-^{13}C]glucose 10 carbon atoms of **6** acquired ^{13}C enrichment with an average ^{13}C abundance of 3.8 ± 0.6% ^{13}C, whereas the remaining positions had a ^{13}C abundance of 1.1 ± 0.1% ^{13}C, i.e. in the natural abundance range (Table 3, Fig. 5B). A very similar situation was found in compound **7**, where 10 labeled carbon atoms had an

Table 1. ^{13}C NMR and ^{1}H NMR data of cannabichromenic acid (6). *, Second hydrogen atom of a diastereotopic pair.

	Chemical shift (p.p.m.)		Coupling constants (Hz)		Correlation pattern			
Position	^{13}C	^{1}H	J_{HH}	J_{CC}[a]	DQF-COSY	NOESY	HMBC	INADEQUATE[b]
1	116.69	5.46 (d)	10.1	68.3 (2)	2, 5′ (w)[c]			2
2	126.32	6.72 (d)	10.1	68.1 (1)	1	4, 4*, 5 3-Me	3-Me	1
3	80.00			40.5 (3-Me)			3-Me	3-Me
4	41.68	1.64 (m)		37.4	4*, 5	2, 4*, 5, 6 3-Me	3-Me	
4*		1.76 (m)			4, 5	2, 4, 5, 6, 3-Me		
5	22.65	2.08 (m)		44.0 (6), 4.4 (8)	4, 4*	2, 4, 4*, 6 9, 3-Me	9	6
6	123.86	5.07 (t)	6.9	44.0 (5) 3.3 (8)	4, 4*, 5	4, 4*, 5	5, 8, 9	5
7	131.84			42.2 (9)			5, 8, 9	9
8	25.64	1.64 (s)		3 (6), 4 (5)		9	9	
9	17.60	1.55 (s)		42.0 (7)		8	8	7
3-Me	27.14	1.39 (s)		40.7 (3)		2, 4, 4*, 5		3
1′	107.09			73.0 (2′)			1, 5′, OH	2′
2′	160.63			73.2 (1′)			OH	1′
3′	102.94			74.3 (COOH)			5′, 1′′, OH	COOH
4′	149.50			42,0 (1′′)			1′′	1′′
5′	111.49	6.22 (s)		67.4 (6′)	1 (w)		1′′	6′
6′	158.97			67.4 (5′)			5′	5′
1′′	36.75	2.86 (dd)	7.9, 9.8	42 (4′)	2′′	2′′, 3′′, 4′′ OH	5′	4′
2′′	31.30	1.56 (m)		34.5 (3′′)		1′′, 3′′, 4′′, OH	1′′, 3′′, 4′′, 5′′	3′′
3′′	31.98	1.33 (m)		34.3 (2′′)	2′′	1′′, 2′′, OH		2′′
4′′	22.46	1.33 (m)		34.7 (5′′)	5′′	1′′, 2′′, OH	5′′	5′′
5	14.02	0.88 (t)	6.8	34.7 (4)	4′′			4′′
OH (2′)		11.70 (s)				2, 1′′, 2′′ 3′′, 4′′		
COOH	176.10			74.3 (3′)				3′

[a] Detected in the ^{13}C NMR spectrum of the sample from the experiment with [U-$^{13}C_6$]glucose. ^{13}C coupled carbon atoms are indicated in parentheses. [b] From the ^{13}C-labeled sample. [c] w, weak cross-peak intensity.

average ^{13}C abundance of 3.2 ± 0.3% ^{13}C and the 12 nonlabeled carbon atoms had an abundance of 1.2 ± 0.1% ^{13}C (Table 3, Fig. 5B). As explained in detail below, the observed distribution of ^{13}C labels provides unequivocal evidence for a nonmevalonate origin of the terpenoid moiety and for a polyketide origin of the phenolic moiety.

The central intermediary metabolism has been found to be similar in a wide variety of higher plants [19–22]. On the basis of these data, labeling patterns can be predicted for IPP and DMAPP formed via the mevalonate or deoxyxylulose pathway origin, respectively (Figs 6 and 7). A comparison of these hypothetical predictions with the experimentally observed labeling patterns show that the cannabinoids under study are derived entirely or predominantly (> 98%) from the deoxyxylulose pathway. It should be noted that the predicted $^{13}C_3$ isotopomer in IPP and DMAPP formed via the deoxyxylulose route was only detected in the DMAPP derived moiety of compound **6** (Fig. 7). $^{13}C_3$ isotopomers could not be observed in compound **7 and** the IPP derived moiety of **6** because of long-range coupling constants below the detection limit.

The prediction of hypothetical labeling patterns of the hexylphenolic moiety of **6** and **7** via a polyketide mechanism with acetyl-CoA as starter unit and five molecules of malonyl-CoA perfectly matched the detected labeling patterns (Fig. 8). These data confirm earlier hypotheses [7].

As the deoxyxylulose phosphate pathway of IPP, DMAPP and geranyl diphosphate biosynthesis is operative in the plastid compartment of plant cells [15,16,23,24] it appears probable that cannabinoids are biosynthesized in the plastid compartments of *Cannabis* glandular trichomes.

The compartmental separation of the mevalonate pathway and the deoxyxylulose pathway is not absolute [12]. At least one common metabolite can be exchanged between the compartmental boundaries. Thus, the earlier observed incorporation of radioactively labeled mevalonate into cannabinoids [7] might reflect a minor contribution of

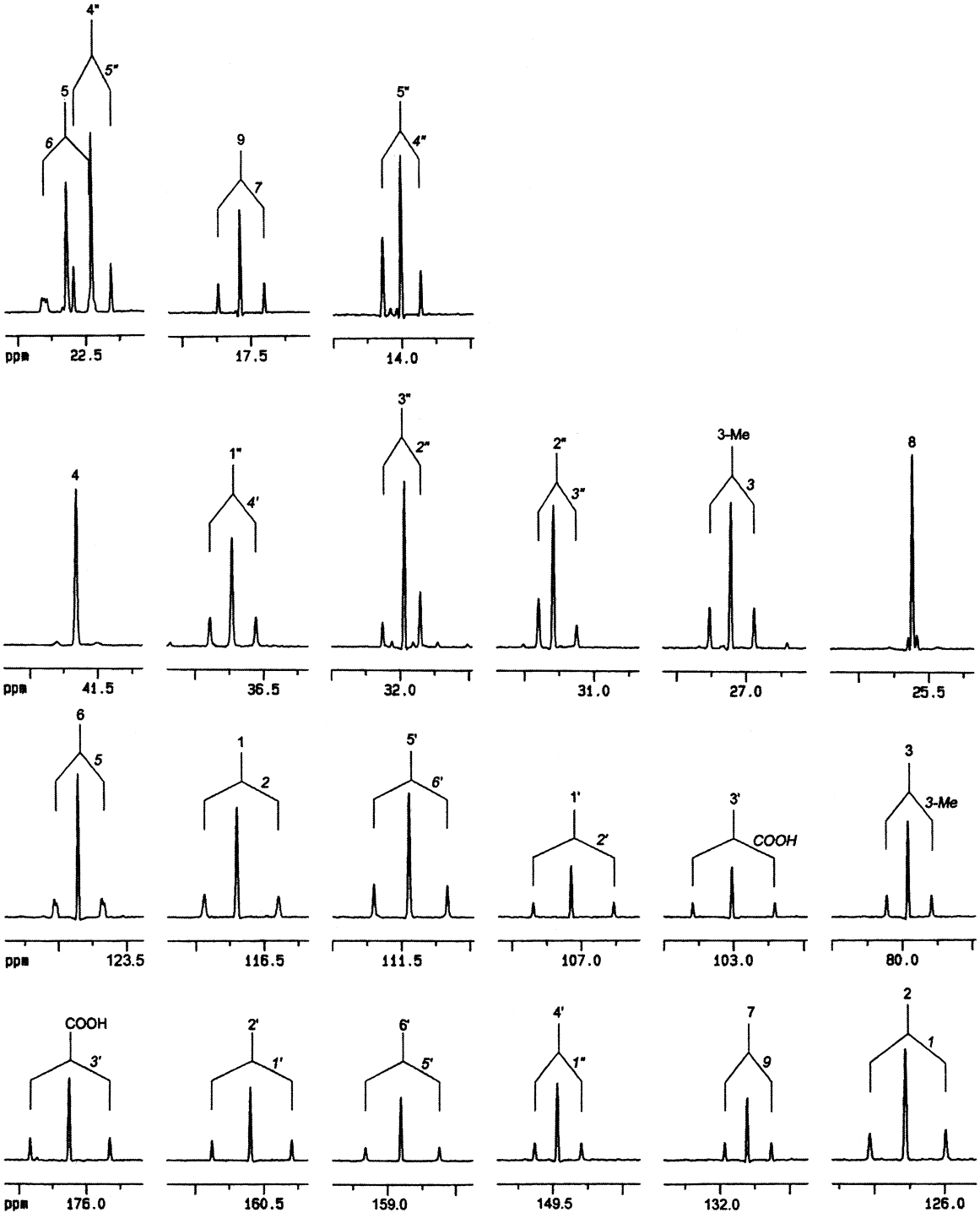

Fig. 3. ^{13}C NMR signals of cannabichromenic acid (6) from the experiment with [U-$^{13}C_6$]glucose.

Table 2. ^{13}C-NMR-und ^{1}H-NMR data of tetrahydrocannabinolic acid (7). *, Second hydrogen atom of a diastereotopic pair.

	Chemical shift,		Coupling constants, Hz		Correlation pattern			
Position	^{13}C	^{1}H	J_{HH}	J_{CC}[a]	DQF-COSY	NOESY	HMBC	INADEQUATE[c]
1	33.40	3.21 (d)	11.2	42.5 (2)	2, 4, 6,	2, 8 (w)[b],	5*, 6	2
2	123.61	6.38 (s)		42.0 (1)	3-Me	9, 3-Me	3-Me	1
					Me	9, 3-Me		
					1, 4, 3-Me	1, 3-Me		
3	133.62			43.6 (3-Me)			4, 5*, 3-Me	3-Me
4	31.14	2.14 (m)			1, 5, 5*,	5, 5*, 8,	3-Me	
					3-Me	3-Me		
5	24.93	1.42 (m)		33.8 (6)	4, 5*	4, 5*, 6	4, 6	6
5*		1.89 (m)			4, 5	4, 5, 6		
6	45.53	1.67 (m)		34.1 (5)	1, 8	5, 5*,8	8, 9	5
7	78.75			38.7 (9)			6, 8, 9	9
8	27.28	1.42 (s)			9	1 (w), 9,6	9	
9	19.43	1.09 (s)		38.5 (7)	8	1, 8	6, 8	7
3-Me	23.25	1.66 (s)		43.6 (3)	1, 2	1, 2, 4	4	3
1′	109.80			71.2 (2′)			5′, OH	2′
2′	164.65			71.0 (1′)			OH	1′
3′	102.32			74.1			5′, 1′′, 1′′*,	COOH
				(COOH)			OH	
4′	146.96			42.2 (1′′)			1′′, 1′′*	1′′
5′	112.63	6.24 (s)		66.1 (6′)		1′′, 1′′*,	1′′, 1′′*	6′
						2′′, 3′′, 4′′		
6′	159.74			66.1 (5′)			5′	5′
1′′	36.44	2.77 (dq)	15.8, 9.8,	42.3 (4′)	1′′*, 2′′	5′, 2′′,	2′′, 3′′	4′
			6.2			3′′, 4′′		
1′′*		2.93 (dq)	15.5, 9.3,		2′′, 1′′	5′, 2′′,		
			6.1			3′′, 4′′		
2′′	31.19	1.57 (m)		34.3 (3′′)	1′′, 1′′*,	5′, 1′′, 1′′*,	1′′, 1′′*,	3′′
					3′′	3′′, 4′′	3′′	
3′′	31.97	1.34 (m)		34.5 (2′′)	2′′	5′, 1′′, 1′′*,	1′′, 1′′*, 2′′,	2′′
						2′′, 5′′	4′′, 5′′	
4′′	22.45	1.34 (m)		34.7 (5′′)	5′′	5′, 1′′, 1′′*,	3′′, 5′′	5′′
						2′′, 5′′		
5′′	13.99	0.89 (t)	6.8	34.5 (4′′)	4′′	2′′, 3′′, 4′′	3′′, 4′′	4′′
OH (2′)′		12.15 (s)				2		
COOH	176.82			74.3 (3′)				

[a]Detected in the ^{13}C NMR spectrum of the sample from the experiment with [U-$^{13}C_6$]glucose. ^{13}C coupled carbon atoms are indicated in parentheses. [b]From the ^{13}C-labeled sample. [c] w, weak cross-peak intensity.

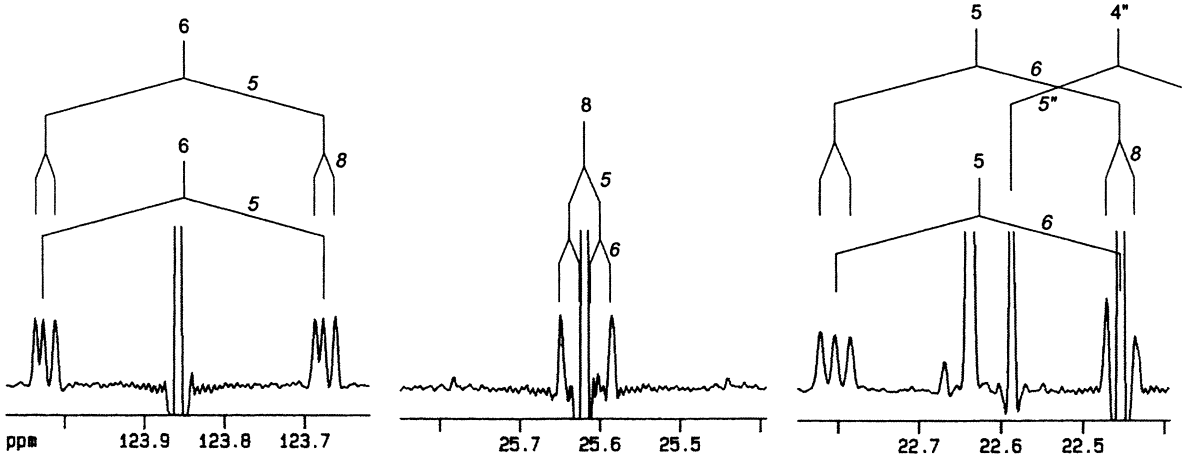

Fig. 4. Expanded view of ^{13}C NMR signals of C-6, C-8 and C-5 of cannabichromenic acid (6) from the experiment with [U-$^{13}C_6$]glucose. ^{13}C coupling patterns are indicated.

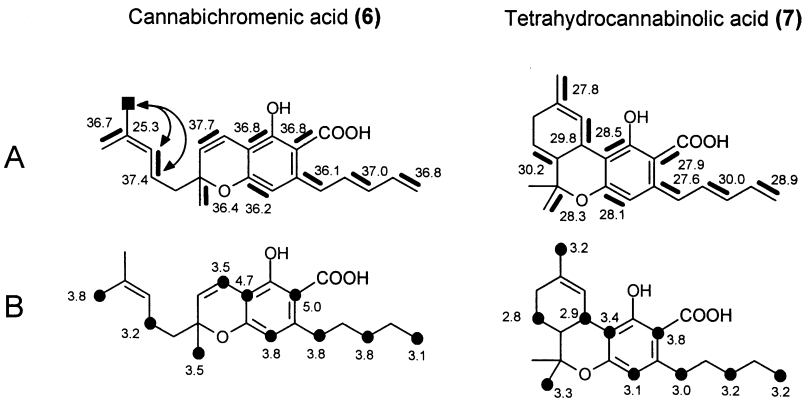

Fig. 5. ^{13}C-labeling patterns of cannabichromenic acid (6) and tetrahydrocannabinolic acid (7)**.** (A) Obtained from the experiment with [U-$^{13}C_6$]glucose; bold lines indicate ^{13}C-labeled isotopomers with directly adjacent ^{13}C atoms, arrows indicate [5,6,8-$^{13}C_3$]**6**, and numbers represent fractions of ^{13}C-coupled satellites in the global NMR signal of a given carbon atom (in percentage). (B) Obtained from the experiment with [1-^{13}C]glucose; filled circles indicate significantly ^{13}C-enriched atoms (> 2.5% ^{13}C) and numbers represent absolute ^{13}C abundances.

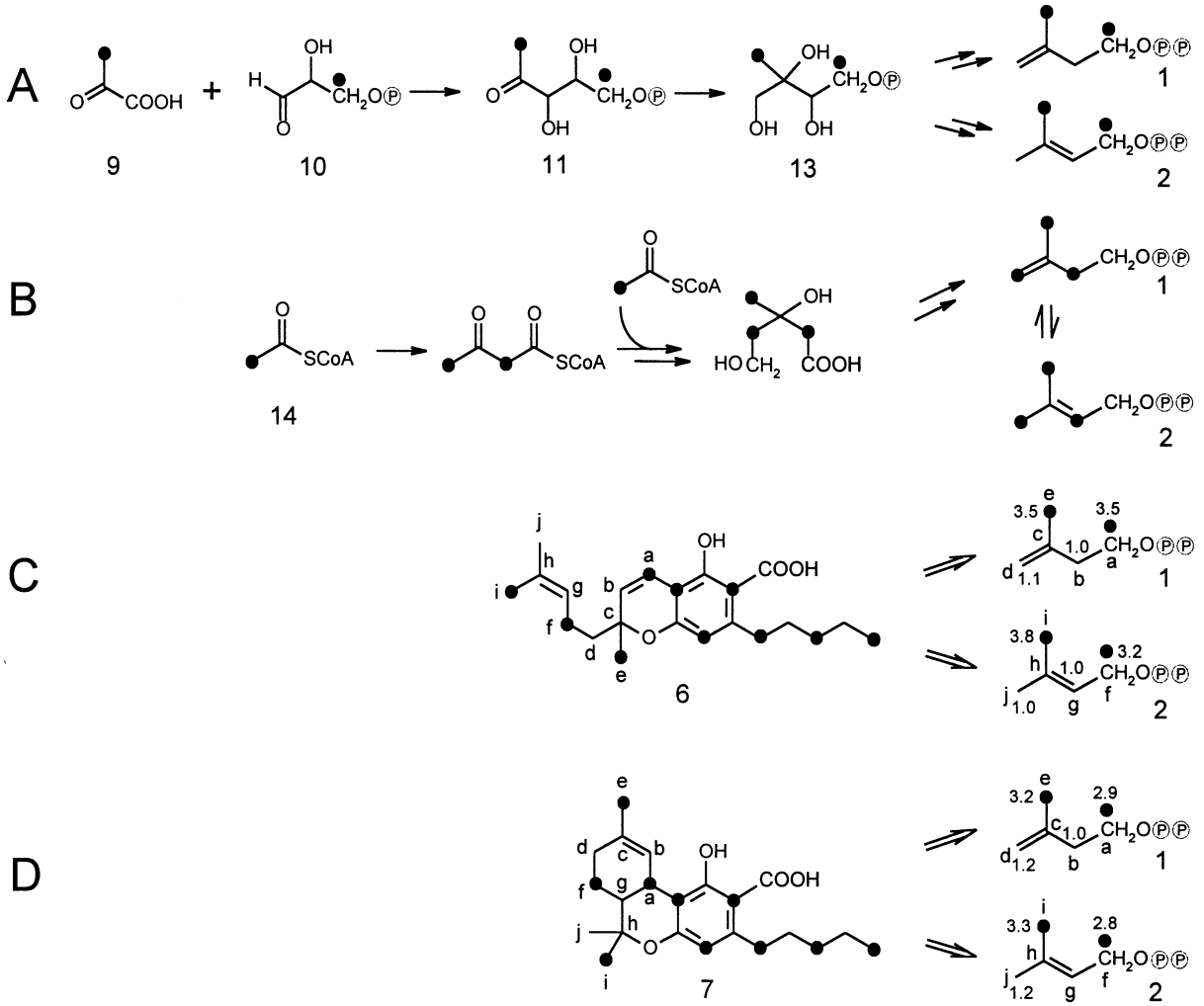

Fig. 6. Labeling patterns for IPP (1) **and DMAPP** (2) **from the experiment with [1-^{13}C]glucose.** Filled circles indicate significantly ^{13}C-enriched atoms (> 2.5% ^{13}C) and numbers represent absolute ^{13}C abundances. (A) Prediction via the deoxyxylulose phosphate pathway of IPP/DMAPP biosynthesis. (B) Prediction via the mevalonate pathway of IPP/DMAPP biosynthesis. The labeling patterns of pyruvate (**9**), glyceraldehyde 3-phosphate (**10**), and acetyl-CoA (**14**) are predicted from published data [19–22]. (C) Reconstruction from the labeling pattern of cannabichromenic acid (**6**). (D) Reconstruction from the labeling pattern of tetrahydrocannabinolic acid (**7**).

Table 3. ^{13}C abundances of cannabichromenic acid (6) and tetrahydrocannabinolic acid (7) from cut sprouts of *C. sativa* proffered with a mixture of [U-$^{13}C_6$]glucose (99.9% ^{13}C enrichment) and unlabeled glucose at a ratio of 1 : 20 (w/w) or with [1-^{13}C]glucose (50% ^{13}C enrichment).

	Compound **6** (% ^{13}C)		Compound **7** (% ^{13}C)	
Position	[1-^{13}C]glucose	[U-$^{13}C_6$]glucose	[1-^{13}C]glucose	[U-$^{13}C_6$]glucose
1	3.5	1.7	2.9	1.5
2	1.0	1.7	1.0	1.4
3	1.2	1.6	1.2	1.6
4	1.1	1.7	1.2	1.5
5	3.2	1.5	2.8	1.5
6	1.0	1.7	1.0	1.5
7	1.3	1.7	1.3	1.8
8	1.0	1.4	1.2	1.5
9	3.8	1.8	3.3	1.5
3-Me	3.5	1.6	3.2	1.5
1′	4.7	2.0	3.4	2.0
2′	1.2	1.6	1.2	1.7
3′	5.0	2.0	3.8	1.9
4′	1.2	1.7	1.3	1.7
5′	3.8	1.7	3.1	1.5
6′	1.3	1.7	1.3	1.6
1′′	3.8	1.7	3.0	1.5
2′′	1.1	1.5	1.1	1.5
3′′	3.8	1.7	3.2	1.6
4′′	1.1	1.5	1.3	1.6
5′′	3.1	1.7	3.2	1.7
COOH	1.1	1.7	1.2	1.6

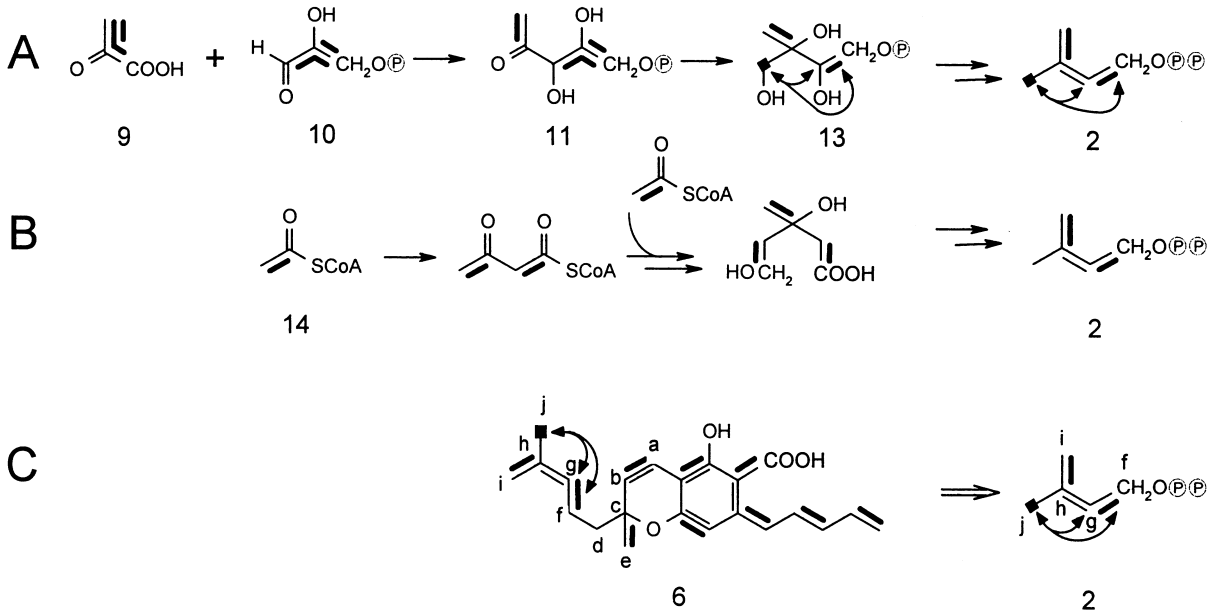

Fig. 7. Labeling patterns for DMAPP (2) from the experiment with [U-$^{13}C_6$]glucose; bold lines indicate ^{13}C labeled isotopomers with directly adjacent ^{13}C atoms, arrows indicate $^{13}C^{13}C$ couplings via multiple bonds. (A) Prediction via the deoxyxylulose phosphate pathway of IPP/DMAPP biosynthesis. (B) Prediction via the mevalonate pathway of IPP/DMAPP biosynthesis. The labeling patterns of pyruvate (**9**), glyceraldehyde 3-phosphate (**10**), and acetyl-CoA (**14**) are predicted from published data [19–22]. (C) Reconstruction from the observed labeling pattern of cannabichromenic acid (**6**).

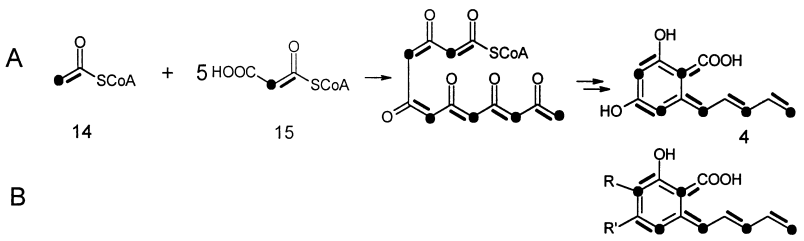

Fig. 8. Biosynthesis of olivetolic acid. (A) Prediction of the labeling pattern of olivetolic acid (**4**) via a polyketide based biosynthetic pathway. The labeling patterns of acetyl-CoA (**14**) and malonyl-CoA (**15**) are predicted from published data [19–22]. Bold lines indicate ^{13}C labeled isotopomers with directly adjacent ^{13}C atoms from [U-$^{13}C_6$]glucose and filled circles indicate ^{13}C-enriched atoms from [1-^{13}C]glucose. (B) Observed labeling patterns in cannabichromenic acid (**6**) and tetrahydrocannabinolic acid (**7**).

mevalonate derived metabolites via cross-talk of the two terpenoid biosynthetic pathways.

ACKNOWLEDGEMENTS

This work was supported by the Deutsche Forschungsgemeinschaft (SFB 369). We thank Fritz Wendling for expert help with the preparation of the manuscript.

REFERENCES

1. Turner, J.C., Hemphill, J.K. & Mahlberg, P.G. (1978) Quantitative determination of cannabinoids in individual glandular trichomes of *Cannabis sativa* L. (Cannabaceae). *Am. J. Bot.* **65**, 1103–1106.
2. Mechoulam, R. (1970) Marihuana chemistry. *Science* **168**, 1159–1166.
3. Devane, W.A., Dysarz, F.A., Johnson, M.R., Melvin, L.S. & Howlett, A.C. (1988) Determination and characterization of a cannabinoid receptor in rat brain. *Mol. Pharmacol.* **34**, 605–613.
4. Di Marzo, V., De Petrocellis, L., Bisogno, T. & Maurelli, S. (1995) Pharmacology and physiology of the endogenous cannabimimetic mediator anandamide. *J. Drug. Dev. Clin. Pract.* **7**, 199–219.
5. Baker, D., Pryce, G., Croxford, J.L., Brown, P., Pertwee, R.G., Huffman, J.W. & Layward, L. (2000) Cannabinoids control spasticity and tremor in a multiple sclerosis model. *Nature* **404**, 84–87.
6. Malfait, A.M., Gallily, R., Sumariwalla, P.F., Malik, A.S., Andreakos, E., Mechoulam, R. & Feldmann, M. (2000) The nonpsychoactive cannabis constituent cannabidiol is an oral anti-arthritic therapeutic in murine collagen-induced arthritis. *Proc. Natl Acad. Sci. USA* **97**, 9561–9566.
7. Shoyama, Y., Yagi, M., Nishioka, I. & Yamauchi, T. (1975) Biosynthesis of cannabinoid acids. *Phytochemistry* **14**, 2189–2192.
8. Fellermeier, M. & Zenk, M.H. (1998) Prenylation of olivetolate by a hemp transferase yields cannabigerolic acid, the precursor of tetrahydrocannabinol. *FEBS Lett.* **427**, 283–285.
9. Taura, F., Morimoto, S. & Shoyama, Y. (1995) First direct evidence for the mechanism of Δ^1-tetrahydrocannabinolic acid biosynthesis. *J. Am. Chem. Soc.* **117**, 9766–9767.
10. Morimoto, S., Komatsu, K., Taura, F. & Shoyama, Y. (1998) Purification and characterization of cannabichromenic acid synthase from *Cannabis sativa*. *Phytochemistry* **49**, 1525–1529.
11. Taura, F., Morimoto, S. & Shoyama, Y. (1996) Purification and characterization of cannabidiolic-acid synthase from *Cannabis sativa*. *J. Biol. Chem.* **271**, 17411–17416.
12. Eisenreich, W., Schwarz, M., Cartayrade, A., Arigoni, D., Zenk, M.H. & Bacher, A. (1998) The deoxyxylulose phosphate pathway of terpenoid biosynthesis in plants and microorganisms. *Chem. Biol.* **5**, R221–R233.
13. Rohmer, M. (1999) The discovery of a mevalonate-independent pathway for isoprenoid biosynthesis in bacteria, algae and higher plants. *Nat. Prod. Report* **16**, 565–574.
14. Herz, S., Wungsintaweekul, J., Schuhr, C.A., Hecht, S., Lüttgen, H., Sagner, S., Fellermeier, M., Eisenreich, W., Zenk, M.H., Bacher, A. & Rohdich, F. (2000) Biosynthesis of terpenoids: YgbB protein converts 4-diphosphocytidyl-2C-methyl-D-erythritol 2-phosphate to 2C-methyl-D-erythritol 2,4-cyclodiphosphate. *Proc. Natl Acad. Sci. USA* **97**, 2486–2490.
15. Arigoni, D., Sagner, S., Latzel, C., Eisenreich, W., Bacher, A. & Zenk, M.H. (1997) Terpene biosynthesis from 1-deoxy-D-xylulose in higher plants by intramolecular skeletal rearrangement. *Proc. Natl Acad. Sci. USA* **94**, 10600–10605.
16. Schwender, J., Zeidler, J., Groner, R., Muller, C., Focke, M., Braun, S., Lichtenthaler, F.W. & Lichtenthaler, H.K. (1997) Incorporation of 1-deoxy-D-xylulose into isoprene and phytol by higher plants and algae. *FEBS Lett.* **414**, 129–134.
17. Bacher, A., Rieder, C., Eichinger, D., Arigoni, D., Fuchs, G. & Eisenreich, W. (1999) Elucidation of novel biosynthetic pathways and metabolite flux patterns by retrobiosynthetic NMR analysis. *FEMS Microbiol. Rev.* **22**, 567–598.
18. Bacher, A. & Eisenreich, W. (2001) Application of isotopes in investigating biosynthetic pathways. In *Synthesis and Applications of Isotopically Labelled Compounds*, Vol. 7. Wiley, New York, in press.
19. Eisenreich, W., Rieder, C., Grammes, C., Heßler, G., Adam, K.-P., Becker, H., Arigoni, D. & Bacher, A. (1999) Biosynthesis of a neo-*epi*-verrucosane diterpene in the liverwort *Fossombronia alaskana*. A retrobiosynthetic NMR study. *J. Biol. Chem.* **274**, 36312–36320.
20. Eichinger, D., Bacher, A., Zenk, M.H. & Eisenreich, W. (1999) Quantitative assessment of metabolic flux by ^{13}C NMR analysis. Biosynthesis of anthraquinones in *Rubia tinctorum*. *J. Am. Chem. Soc.* **121**, 7469–7475.
21. Goese, M., Kammhuber, K., Bacher, A., Zenk, M.H. & Eisenreich, W. (1999) Biosynthesis of bitter acids in hop. A ^{13}C and ^{2}H NMR study on the building blocks of humulone. *Eur. J. Biochem.* **263**, 447–454.
22. Werner, I., Bacher, A. & Eisenreich, W. (1997) Formation of gallic acid in plants and fungi. A retrobiosynthetic study with ^{13}C-labeled glucose. *J. Biol. Chem.* **272**, 25474–25482.
23. Burke, C.C., Wildung, M.R. & Croteau, R. (1999) Geranyl diphosphate synthase: cloning, expression, and characterization of this prenyltransferase as a heterodimer. *Proc. Natl Acad. Sci. USA* **96**, 13062–13067.
24. Turner, G., Gershenzon, J., Nielson, E.E., Froehlich, J.E. & Croteau, R. (1999) Limonene synthase, the enzyme responsible for mooterpene biosynthesis in peppermint, is localized to leucoplasts of oil gland secretory cells. *Plant Physiol.* **120**, 879–886.